24th International Conference on Renewable Energies and Power Quality (ICREPQ'26)
Santander (Spain), 10th to 12th June 2026
ISBN-13: 978-84-09-82044-3

Small-signal stability study of grid-connected voltage source converters with grid-forming control

L. Sainz de Ezquerra[1], J. Pedra[1], Ll. Monjo[2], J.J. Mesas[1], O. Cartiel[1] and L. Sainz[1]

[1] Department of Electrical Engineering (DEE)
Escola Tècnica Superior d'Enginyeria Industrial de Barcelona (ETSEIB)
Universitat Politècnica de Catalunya – BarcelonaTech (UPC)
Av. Diagonal 647, 08028 Barcelona (Spain)

[2] Department of Electrical Engineering (DEE)
Escola Politècnica Superior d'Enginyeria de Vilanova i la Geltrú (EPSEVG)
Universitat Politècnica de Catalunya – BarcelonaTech (UPC)
Av. Victor Balaguer 1, 08800 Vilanova i La Geltrú (Spain)

Abstract. The large-scale integration of renewable energy sources is transforming traditional power grids. Renewable generation is typically connected to distribution networks through voltage source converters (VSCs) operating under grid-following (GFL) control, which has raised technical concerns regarding system stability and security. Grid-forming (GFM) VSCs are emerging as a solution, capable of establishing a grid and operating in parallel with other devices via self-synchronisation mechanisms. However, they introduce new challenges, particularly small-signal stability issues arising from interactions with traditional power-system components. Research on GFM VSC stability is still at an early stages, despite its key role in transmission networks and large-scale renewable plants. Stability studies often rely on time-domain simulations and frequency-domain approaches using white- and black-box admittance models of system components. This paper presents a small-signal stability analysis of grid-connected VSCs under GFM control strategies, including power synchronisation control (PSC) and alternating voltage control (AVC). The analysis is conducted using Simulink-based time-domain simulations and frequency-domain methods based on black-box GFM VSC models.

Key words. Grid-connected voltage source converter, grid-forming control, time-domain simulations, black-box models, stability assessment, small-signal modelling.

1. Introduction

Traditional power systems (PSs) have historically followed a centralised architecture based on large-scale power generation plants connected to transmission grids through synchronous generators [1], [2]. Since the early 20th century, the increasing global demand for clean and efficient energy has reshaped PS architectures, leading to the deployment of renewable energy resources [3]. These resources are essential for achieving sustainable and decarbonised energy systems, but their large-scale integration is transforming the traditional PS paradigm [3], [4]. Renewable generation is predominantly integrated into distribution grids through VSCs operating under GFL control. However, GFL VSCs have been associated with several technical concerns, as highlighted by recent events such as the Iberian blackout [5], which imposes constraints on the penetration of renewable energy resources. To address these issues, GFM control strategies such as droop, power synchronisation, virtual synchronous generator, matching, and other more complex controls [6], [7], which are mainly based on power synchronisation control (PSC) and alternating voltage control approaches (AVC) have been proposed in the literature. GFM VSCs are emerging as a promising technology for transmission grids with large-scale renewable plants. However, they also introduce new small-signal stability challenges arising from interactions between converter-based devices and traditional PS components.

Previous studies on GFM VSC stability have mostly performed numerical analysis, concluding that PSC can provoke instabilities near to synchronous frequency in weak grids [8], [9], while AVC can influence PSC dynamics [10], [11]. Furthermore, sub-synchronous oscillations have been reported in weak grids when current control (CC) is combined with AVC [12]. In [13], a comprehensive analytical framework is developed to evaluate the stability of GFM VSCs providing design-oriented insights for controller tuning. Despite these advances, comprehensive stability studies of AC/DC grid-connected GFM VSCs remain limited, and such studies are essential for modern PS stability analysis under large-scale renewable integration.

Small-signal stability assessment is commonly performed using state-space eigenvalue analysis, closed-loop pole analysis, impedance-based frequency-domain methods, and time-domain simulations. Frequency-domain methods such as the resonance mode analysis (RMA)-based positive-mode-damping (PMD) criterion [14] are increasingly adopted for complex systems, allowing stability evaluation with reduced computational effort and black-box impedance modelling [15]. Time-domain

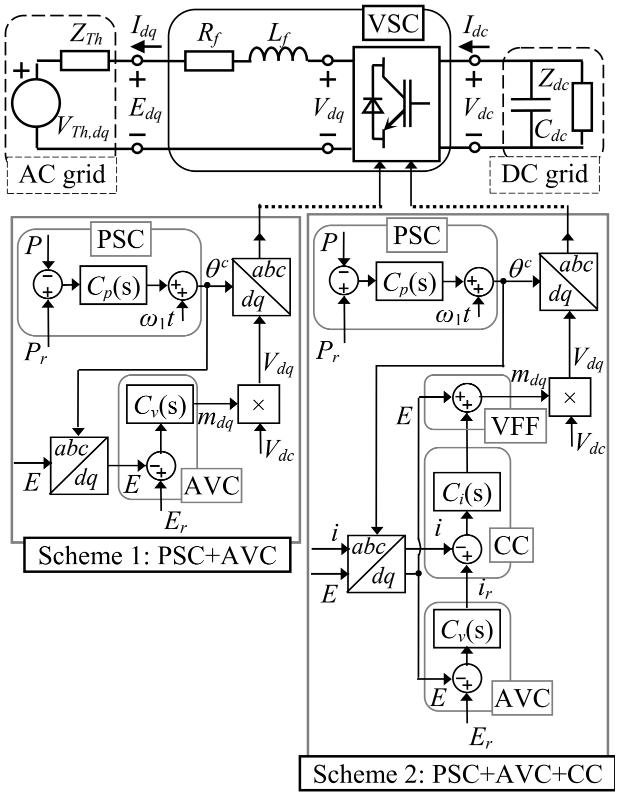

Fig. 2. *DQ*-real single-line diagram of three-phase VSC and GFM control schemes.

simulations are another important tool for analysing and validating stability studies.

This paper presents a small-signal stability analysis of grid-connected GFM VSCs under PSC and AVC strategies. MATLAB/Simulink models of the studied systems are developed to perform time-domain simulations and assess the impact of key control and grid parameters on system stability. In addition, frequency-domain stability analysis is carried out using the RMA-based PMD stability criterion in combination with black-box admittance models of the GFM VSCs. This combined approach enables a systematic evaluation of stability under both AC-only and full AC/DC modelling assumptions, providing deeper insight into the role of AC/DC interactions in converter-dominated power systems.

2. Grid-connected GFM VSC framework

The three-phase grid-connected GFM VSC, together with the two main GFM control strategies in [13], is analysed. Fig. 1 shows the *dq*-real single-line diagram of the three-phase grid-connected VSC. An *L*-type filter, defined by the inductance L_f and the equivalent series resistance R_f, is considered on the AC side of the VSC, while the DC-side voltage is assumed to be variable. The AC side of the VSC is connected to the AC grid, modelled by a Thevenin-equivalent circuit with $V_{Th,\,dq}$ and Z_{Th}, whereas the DC side is connected to a *C*-type filter, defined by the capacitance C_{dc}, and a DC load characterised by an equivalent impedance Z_{dc}. The two main GFM control schemes from [13] are implemented: (i) Scheme 1: PSC + AVC; (ii) Scheme 2: PSC + AVC + CC. These schemes consider the PSC, AVC, CC, and voltage feedforward (VFF). Each control block performs a specific role within the overall control structure, as detailed below:

- The PSC regulates the system frequency by emulating the $p-f$ droop characteristic of synchronous generators using an integral (I) controller expressed as $C_p(s) = k_p/s$, where k_p denotes the integral gain.
- The AVC regulates the AC voltage using a proportional-integral (PI) controller expressed as $C_v(s) = G_a + k_i/s$, where G_a and k_i denote the proportional and integral gains, respectively.
- The CC and VFF regulate the fast-current dynamics under fault conditions. The CC is implemented as a PI controller with a small integral gain, which is commonly neglected; therefore, the controller is approximated by $C_i(s) = R_a$.

The corresponding circuits are implemented in Simulink to investigate the influence of the GFM VSC parameters on small-signal stability through time-domain simulations. In addition, black-box models of the GFM VSC under the two control strategies are obtained from numerical measurements and employed for stability assessment using the PMD stability criterion [14].

3. GFM VSC modelling

MATLAB/Simulink-based and black-box models are presented for time- and frequency-domain stability

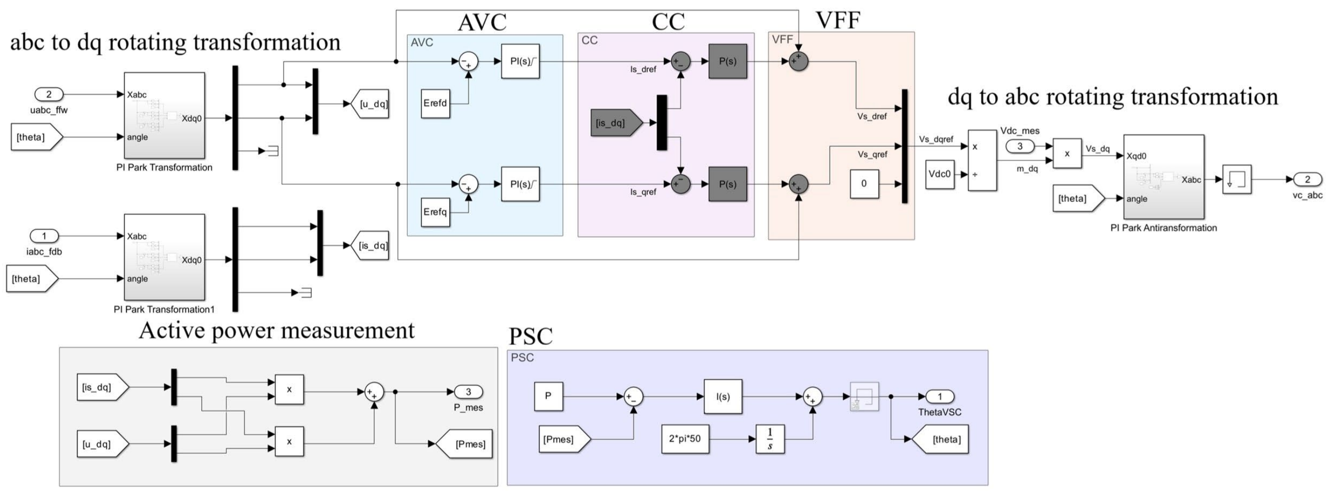

Fig. 1. MATLAB/Simulink model of the control Scheme 2 (PSC + AVC + CC strategy) of the GFM VSC.

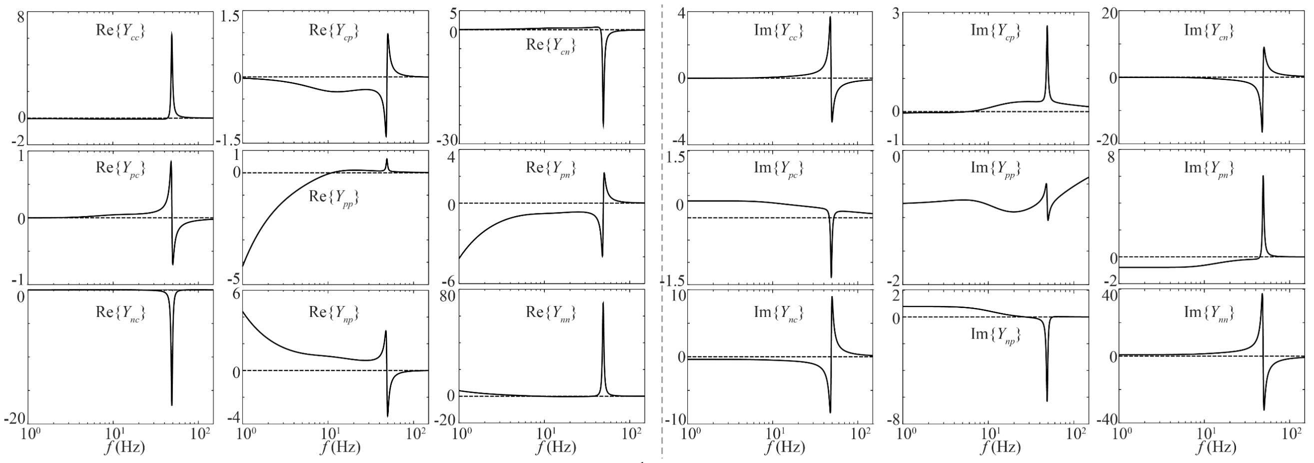

Fig. 3. Black-box characterisation of an AC/DC GFM VSC (in Ω^{-1}) with control Scheme 1: Real (left) and imaginary (right) parts of the frequency-dependent admittance matrix elements obtained from MATLAB/Simulink-based simulations using SARA [15].

studies, respectively. In particular, the two GFM control schemes presented in Fig. 1 are studied using both modelling approaches.

A. MATLAB/Simulink models

A MATLAB/Simulink model is implemented according to the single-line diagram of the three-phase VSC and GFM control schemes in Fig. 1. As an example, Fig. 2 shows the MATLAB/Simulink model of control Scheme 2 with the PSC + AVC + CC strategy.

In this strategy, the PSC regulates the system frequency using an integral (I) controller denoted as $C_p(s)$, based on active power measurements; the corresponding measurement block is also included in the control model. The control is performed in the *dq*-real reference frame, and therefore the *abc*-to-*dq* and *dq*-to-*abc* transformation blocks are also included in the model. Furthermore, the AVC regulates the AC-side voltage at the PCC using a proportional-integral (PI) controller denoted as $C_v(s)$. To this end, this voltage is measured and transformed to the *dq*-real reference frame. This transformed voltage is processed by the AVC which provides the converter reference current. Subsequently, the modulation function is generated by the CC based on the converter reference current. The AC-side internal voltage setpoint of the VSC is finally derived from the reference voltage obtained from the modulation function, the DC-side voltage and the AC-side VFF value at the PCC. This internal voltage is transformed to the *abc*-frame using the *dq*-to-*abc* rotating transformation block.

The MATLAB/Simulink models of the AC/DC grid, the VSC circuit, and Scheme 1 with the PSC + AVC strategy are omitted for brevity, but they follow a similar structure to that shown in the single-line diagram and control blocks of Fig. 1. In particular, the PSC + AVC block is equivalent to the PSC + AVC + CC block without the CC and VFF.

B. Black-box models

The small-signal dynamic behaviour of *dq*-complex voltages and currents in AC/DC electrical devices (e.g., GFL and GFM VSCs and MMCs) can be expressed in the frequency-domain by applying Ohm's law as [15]:

$$\begin{bmatrix} \Delta I_{dc} \\ \Delta \mathbf{I_{dq}} \\ \Delta \mathbf{I^*_{dq}} \end{bmatrix} = \underbrace{\begin{bmatrix} Y_{cc} & Y_{cp} & Y_{cn} \\ Y_{pc} & Y_{pp} & Y_{pn} \\ Y_{nc} & Y_{np} & Y_{nn} \end{bmatrix}_{\omega}}_{\mathbf{Y^{AC/DC}}(\omega)} \begin{bmatrix} \Delta V_{dc} \\ \Delta \mathbf{E_{dq}} \\ \Delta \mathbf{E^*_{dq}} \end{bmatrix}, \quad (1)$$

where $\mathbf{Y^{AC/DC}}(\omega)$ is the small-signal AC/DC admittance matrix of the electrical device; $\mathbf{E_{dq}}$ and $\mathbf{I_{dq}}$ are the *dq*-complex voltage and current space vectors at the AC terminals; V_{dc} and I_{dc} are the DC-side voltage and current; and the symbol Δ denotes small-signal variables.

The characterisation of the AC/DC admittance matrix in (1) by using black-box models of electrical devices in the frequency-domain is a common scenario in industrial applications where Simulink-based implementations are distributed in protected format for intellectual property reasons. In such cases, neither the internal control loops nor the mathematical formulation is accessible, making analytical admittance derivation infeasible. Even in research settings, obtaining closed-form expressions for the full small-signal AC/DC admittance matrix of power-electronic devices may be algebraically complex or computationally cumbersome, thereby motivating frequency-domain black-box identification. This characterisation is performed in this paper using the GFM VSC MATLAB/Simulink model and the MATLAB/Simulink SARA (Simulation-based

Table I. Three-phase grid-connected GFM VSC parameters

	Parameters	Scheme 1 / 2 values	Stability study
AC grid	AC rated voltage E	190 V_{ac}	---
	Rated power P	5 kW	---
	SCR	10 p.u.	Scheme 2
	Frequency, ω_1	314 s^{-1}	---
DC grid	DC rated voltage V_{dc}	380 V_{dc}	---
	R_{dc}, L_{dc}	0.1 Ω, 1 mH	---
	C_{dc}	600 μF	---
GFM VSC	R_f, L_f	189 mΩ, 3 mH	---
	k_p	0.03ω_1 p.u.	Scheme 1
	G_a	0.5 / 3 p.u.	Scheme 1
	k_i	50 / 100 p.u.	---
	R_a	--- / 0.865 p.u.	---

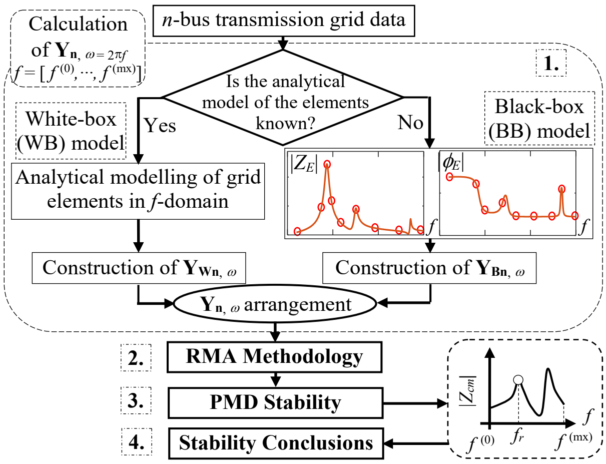

Fig. 4. Flowchart of RMA-based PMD stability criterion.

Admittance Response Analysis) tool. It is worth noting that, at subsynchronous frequencies, the discretisation must be sufficiently fine to accurately capture the frequency response curve and avoid missing relevant features. Moreover, the real and imaginary parts of the admittances are required for the correct application of the black-box modelling approach. As an example, Fig. 3 shows the admittance matrix of the GFM VSC black-box model with the control Scheme 1 (i.e., PSC + AVC strategy) under the parameters listed in Table I.

4. RMA-based PMD stability criterion

RMA is formulated based on the eigenvalue decomposition of the nodal admittance matrix derived from the voltage node method at each frequency ω within a frequency-scan range, i.e., [14]

$$\mathbf{V}_{\mathbf{B},\omega}=\mathbf{Y}_{\mathbf{B},\omega}^{-1}\mathbf{I}_{\mathbf{B},\omega}\ \Rightarrow\ \mathbf{U}_{\omega}=\mathbf{\Lambda}_{\mathbf{Y},\omega}^{-1}\mathbf{J}_{\omega}$$
$$\mathbf{\Lambda}_{\mathbf{Y},\omega}=\begin{bmatrix}\lambda_{Y1} & \cdots & 0\\ \vdots & \ddots & \vdots\\ 0 & \cdots & \lambda_{Yn}\end{bmatrix}_{\omega}=\mathbf{L}_{\omega}\mathbf{Y}_{\mathbf{B},\omega}\mathbf{R}_{\omega},\tag{2}$$

where n is the number of grid buses, $\mathbf{U}_{\omega}=\mathbf{L}_{\omega}\cdot\mathbf{V}_{\mathbf{B},\,\omega}$, $\mathbf{J}_{\omega}=\mathbf{L}_{\omega}\cdot\mathbf{I}_{\mathbf{B},\,\omega}$ are the modal voltage and current vectors, respectively, and $\mathbf{\Lambda}_{\mathbf{Y},\,\omega}$, is the diagonal eigenvalue matrix of $\mathbf{Y}_{\mathbf{B},\,\omega}$ at frequency ω. In addition, $\mathbf{R}_{\omega}$ and $\mathbf{L}_{\omega}$ represent the right (column-wise) and left (row-wise) eigenvector matrices, respectively. Singularities in the nodal admittance matrix $\mathbf{Y}_{\mathbf{B},\,\omega}$ at resonance frequencies ω_r are directly linked to singular eigenvalues of $\mathbf{\Lambda}_{\mathbf{Y},\,\omega}$, referred to as critical resonance modes. These singular eigenvalues manifest as peak values of the eigenvalue magnitudes of $\mathbf{Z}_{\mathbf{B},\,\omega}=(\mathbf{Y}_{\mathbf{B},\,\omega})^{-1}$, i.e., as peaks in the diagonal element magnitudes of $\mathbf{\Lambda}_{\mathbf{Z},\,\omega}=(\mathbf{\Lambda}_{\mathbf{Y},\,\omega})^{-1}=\mathrm{diag}(Z_{m1},\ldots Z_{mn})_{\omega}$, where $Z_{mi,\omega}=1/\lambda_{mi,\omega}$ are the modal impedances that characterise the corresponding resonance modes of $\mathbf{Z}_{\mathbf{B},\,\omega}$.

As a powerful alternative to the GNC, the RMA is applied within the PMD stability criterion for the frequency-domain stability assessment of multi-terminal AC/DC transmission grids [14]. Grid stability can be assessed by studying every critical resonance mode $Z_{mi,\,\omega}$ at each resonance frequency ω_r and applying the following criterion: the grid is stable if and only if the following condition holds

$$m_{xi,\omega_r}\cdot R_{mi,\omega_r}<0,\tag{3}$$

at all resonance frequencies ω_r (i.e., at frequencies of all local maxima or peak values of $|Z_{mi,\,\omega}|$), where $R_{mi,\,\omega}$ denotes the real component of the critical resonance mode and $m_{xi,\,\omega}$ is the slope of its imaginary part $X_{mi,\,\omega}$ with respect to frequency ω. Fig. 4 summarises the flowchart adopted for the stability analysis.

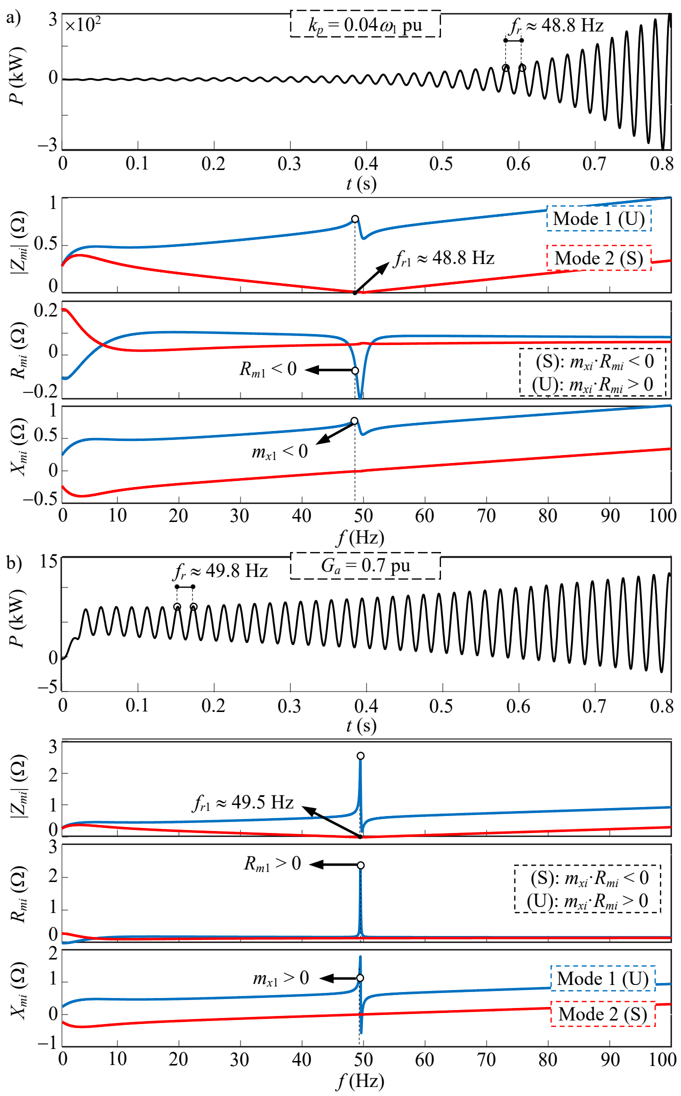

Fig. 5. Stability study of Scheme 1 under AC-only scenario using MATLAB/Simulink simulations (top) and RMA-based PMD stability criterion (bottom): a) k_p influence; b) G_a influence.

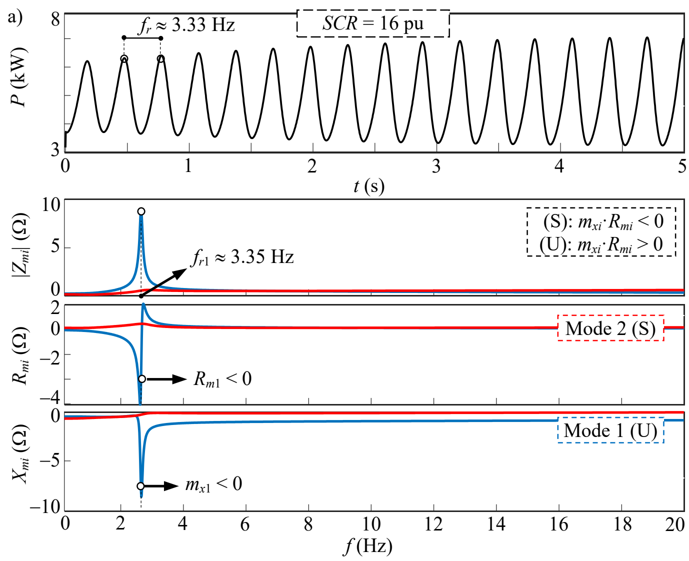

Fig. 6. Stability study of Scheme 2 under AC-only scenario using MATLAB/Simulink simulations (top) and RMA-based PMD stability criterion (bottom): a) SCR influence.

5. Results

Starting from a stable operating condition presented in [13] and defined by the values in Table I, the impact of different parameters on the stability of the grid-connected GFM VSC in Fig. 1 is analysed for both control schemes 1 and 2, considering either the AC-side only (assuming a constant DC-side voltage) or the full AC/DC interaction (with the DC-side voltage determined by the DC circuit). The AC-side grid is characterised by a three-phase voltage source and three-phase pure inductances L_g defined by the short-circuit ratio $SCR = 1/(L_g \cdot \omega_1)$, see Table I. The DC-side grid is characterised by a constant DC-voltage source V_{dc} in the AC-only assumption, and by a capacitance C_{dc}, a DC cable, defined by the inductance L_{dc} and the equivalent series resistance R_{dc}, in series with a constant DC voltage source V_{dc} in the AC/DC assumption, see Table I. The stability scenarios listed in the "Stability study" column of Table I are evaluated under both AC-only and AC/DC assumptions.

A. AC-only assumption

Under the AC-only assumption, [13] predicts that increasing in k_p and G_a degrade synchronous stability in Scheme 1, while increasing in SCR degrades subsynchronous stability in Scheme 2. This behaviour is illustrated in Fig. 4 and Fig. 5 for Scheme 1 and Scheme 2, respectively. This is confirmed by both time-domain MATLAB/Simulink simulations and the frequency-domain RMA-based PMD stability criterion applied to a GFM VSC black-box model (see Fig. 3). In particular, two oscillatory modes (Mode 1 and Mode 2) characterise system stability, and instabilities are observed when the above parameters are increased up to $k_p \approx 0.04\omega_1$ p.u. (Mode 1 at $f_r = 48.8$ Hz) and $G_a \approx 0.7$ p.u. (Mode 1 at $f_r = 49.5$ Hz) in Scheme 1, and $SCR \approx 16$ p.u. (Mode 1 at $f_r = 3.35$ Hz) in Scheme 2.

B. AC/DC assumption

The AC/DC assumption is not considered in [13] and, in general, most GFM VSC studies neglect this assumption. The GFM VSC behaviour when k_p and G_a are increased in Scheme 1, and when SCR is increased in Scheme 2, is illustrated by both time-domain MATLAB/Simulink simulations and the frequency-domain RMA-based PMD stability criterion applied to a GFM VSC black-box model (see Fig. 3) as shown in Fig. 6 and Fig. 7, respectively. It is observed that

- A new mode (Mode 3), in addition to the AC-only assumption modes (Modes 1 and 2), emerges when the AC/DC assumption is considered and significantly influences system stability. This mode is related to the influence of the DC grid on stability.
- In Scheme 1, there is an AC/DC interaction, and Mode 3 (DC grid) strongly affects the AC/DC system dynamics. The frequency response of Modes 1 and 2 is modified by DC interaction, and instability is driven by Mode 3 (rather than Mode 1 as suggested in Subsection 5.A). This instability shifts from 48 – 49 Hz under the AC-only assumption to 61 – 64 Hz when the AC/DC assumption is considered. In this case, the DC-side grid should not be modeled by a constant voltage source in stability studies, in order to avoid neglecting AC/DC interactions.
- In Scheme 2, AC/DC interactions and Mode 3 (associated with the DC grid) have only a minor impact

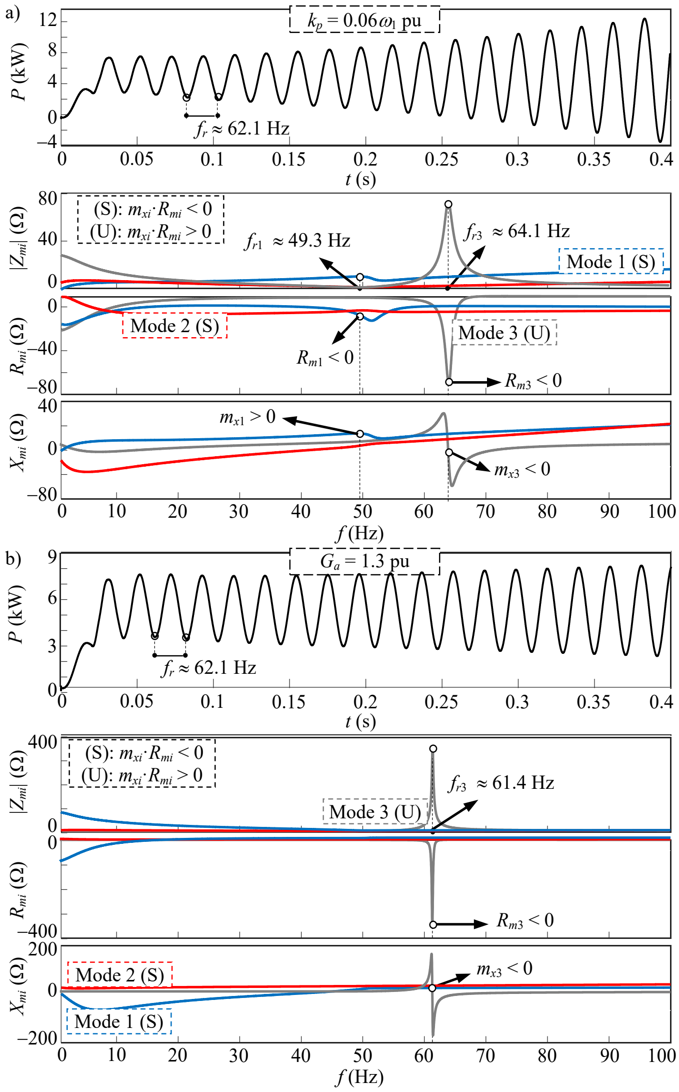

Fig. 7. Stability study of Scheme 1 under AC/DC scenario using MATLAB/Simulink simulations (top) and RMA-based PMD stability criterion (bottom): a) k_p influence; b) G_a influence.

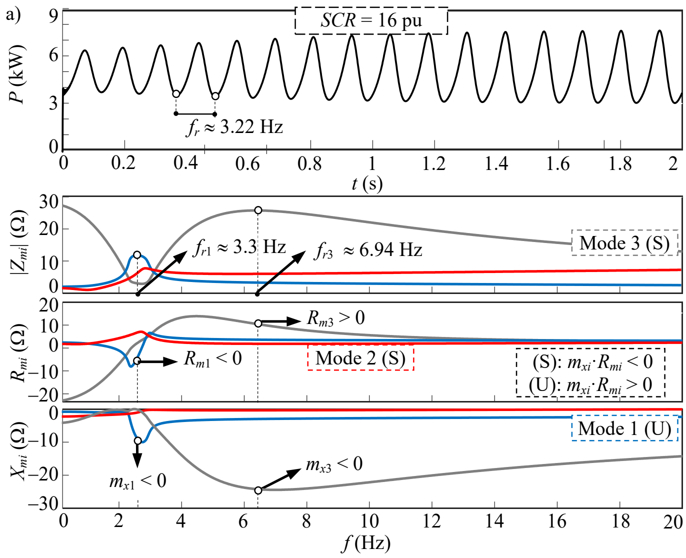

Fig. 8. Stability study of Scheme 2 under AC/DC scenario using MATLAB/Simulink simulations (top) and RMA-based PMD stability criterion (bottom): a) SCR influence.

on the overall AC/DC system dynamics. The frequency response of Modes 1 and 2 is slightly modified by the DC-side interactions, and instability remains driven by Mode 1 at approximately 3.3 Hz. In this case, the DC-side grid may be reasonably approximated as a constant voltage source in stability studies. However, it must be highlighted that Mode 3 (associated with DC-side grid) may still introduce instabilities in the full system.

- In particular, instability is observed when the parameters k_p and G_a in Scheme 1 and SCR in Scheme 2 are increased up to $k_p \approx 0.06\omega_1$ p.u. (Mode 3 at $f_r = 64.1$ Hz) and $G_a \approx 1.3$ p.u. (Mode 3 at $f_r = 61.4$ Hz) in Scheme 1, and $SCR \approx 16$ p.u. (Mode 1 at $f_r = 3.3$ Hz) in Scheme 2.

The results indicate that including DC-side dynamics can significantly affect the stability assessment of grid-connected GFM VSCs, depending on the control scheme. In particular, for Scheme 1, AC/DC interactions introduce an additional mode that becomes the dominant source of instability, which is not captured under the AC-only assumption. Consequently, neglecting the DC grid may lead to inaccurate stability predictions. Therefore, adopting a full AC/DC modelling framework is essential for reliable stability analysis, particularly in systems and control schemes with strong AC/DC coupling.

6. Conclusion

This paper has presented a comprehensive small-signal stability analysis of grid-connected GFM VSCs under PSC- and AVC-based control schemes, considering both AC-only and full AC/DC modelling frameworks. MATLAB/Simulink time-domain models and frequency-domain black-box impedance models have been developed and validated using time-domain simulations and the RMA-based PMD stability criterion.

The results confirm that the AC-only assumption captures the dominant oscillatory modes in simplified scenarios, identifying two main modes associated with synchronous and sub-synchronous dynamics. However, when AC/DC interactions are considered, an additional mode emerges, significantly altering the system stability characteristics. In particular, for the PSC + AVC scheme (Scheme 1), the DC-side dynamics introduce a new dominant mode that governs instability and shifts the oscillatory frequency range. This behaviour is not captured under the AC-only assumption, demonstrating that neglecting DC dynamics may lead to inaccurate stability predictions. In contrast, for the PSC + AVC + CC scheme (Scheme 2), AC/DC interactions have a limited impact on the dominant instability mechanism, although the additional mode may still affect overall system robustness.

These findings highlight that the relevance of AC/DC interactions strongly depends on the control structure. Therefore, the use of simplified AC-only models may be acceptable in some configurations but can be insufficient in others, particularly when strong coupling between AC and DC dynamics exists. Overall, the proposed methodology combining time-domain simulations, black-box modelling, and RMA-based stability assessment provides an effective and practical framework for analysing complex converter-dominated power systems. Black-box modelling is especially suitable for scenarios where detailed internal models are not available, thereby supporting the reliable design and stability assessment of future power systems with high penetration of GFM converters.

Acknowledgement

This work was supported by Ministerio de Ciencia, Innovación y Universidades, FEDER, UE (Grant PID2024-156036OB-C33 supported by MICIU/AEI/10.13039/501100011033/FEDER, UE).

References

[1] P. Kundur, “Power system stability and control,” McGraw-Hill, 1994.

[2] A. Gomez-Exposito, A. J. Conejo, C. Canizares, “Electric Energy Systems: Analysis and Operation,” CRC Press Taylor & Francis Group, 2nd Edition, Taylor & Francis Group LLC, Boca Raton, 2018.

[3] International Renewable Energy Agency (2023). Renewable capacity statistics 2023.

[4] K. Sharifabadi *et al*., Design, Control and Application of Modular Multilevel Converters for HVDC Transmission Systems. Wiley-IEEE press, 2016.

[5] A. Albustami and A. F. Taha, “The Iberian Blackout: A Black Swan or a Gray Rhino? A Thorough Power System Analysis,” arXiv preprint, 2025. [Online]. Available: https://arxiv.org/abs/2511.17433.

[6] M. Chen, *et al*., "Generalized Multivariable Grid-Forming Control Design for Power Converters," in *IEEE Transactions on Smart Grid*, vol. 13, no. 4, pp. 2873-2885, July 2022.

[7] R. Rosso *et al*., “Grid-Forming Converters: Grid-Synchronization, and Future Trends—A Review,” in *IEEE Open J. Ind. Appl*. 2021, 2, 93–109.

[8] L. Zhang, L. Harnefors, and H.-P. Nee, “Power-synchronization control of grid-connected voltage-source converters,” in *IEEE Trans. Power Syst.*, vol. 25, no. 2, pp. 809–820, May 2010.

[9] L. Harnefors *et al.*, “Robust analytic design of power-synchronization control,” in *IEEE Trans. Ind. Electron.*, vol. 66, no. 8, pp. 5810–5819, Aug. 2019.

[10] F. Zhao *et al.*, “Robust grid-forming ontrol with active susceptance,” in *IEEE Trans. Power Electron.*, vol. 38, no. 3, pp. 2872–2877, Mar. 2023.

[11] L. Harnefors *et al.*, “A universal controller for grid-connected voltage-source converters,” in *IEEE J. Emerg. Sel. Topics Power Electron.*, vol. 9, no. 5, pp. 5761–5770, Oct. 2021.

[12] F. Zhao, X. Wang, and T. Zhu, “Power dynamic decoupling control of grid-forming converter in stiff grid,” in *IEEE Trans. Power Electron.*, vol. 37, no. 8, pp. 9073–9088, Aug. 2022.

[13] F. Zhao *et al.*, "Closed-Form Solutions for Grid-Forming Converters: A Design-Oriented Study," in *IEEE Open Journal of Power Electronics*, vol. 5, pp. 186-200, 2024, doi: 10.1109/OJPEL.2024.3357128.

[14] L. Orellana *et al.*, “Stability Assessment for Multi-Infeed Grid-Connected VSCs Modeled in the Admittance Matrix Form,” in *IEEE Transactions on Circuits and Systems I: Regular Papers*, vol. 68, no. 9, pp. 3758-3771, Sept. 2021.

[15] O. Cartiel *et al.*, (2026). SARA (Simulation-based Admittance Response Analysis): A MATLAB/Simulink Tool for AC/DC Admittance Measurement. Zenodo, 2026 doi: https://doi.org/10.5281/zenodo.18245306.